

# Spin Waves and Electronic Interactions in $\text{La}_2\text{CuO}_4$

R. Coldea<sup>1,2</sup>, S.M. Hayden<sup>3</sup>, G. Aeppli<sup>4</sup>, T.G. Perring<sup>2</sup>, C.D. Frost<sup>2</sup>, T.E. Mason<sup>1</sup>, S.-W. Cheong<sup>5</sup>, and Z. Fisk<sup>6</sup>

<sup>1</sup>*Oak Ridge National Laboratory, Oak Ridge, TN 37831, USA*

<sup>2</sup>*ISIS Facility, Rutherford Appleton Laboratory, Chilton, Didcot, OX11 0QX, UK*

<sup>3</sup>*H.H. Wills Physics Laboratory, University of Bristol, Bristol, BS8 1TL, UK*

<sup>4</sup>*NEC Research Institute, Princeton, NJ 08540, USA*

<sup>5</sup>*Lucent Technologies, Murray Hill, NJ 07974, USA*

<sup>6</sup>*Department of Physics, Florida State University, Tallahassee, Florida 32306, USA*

(20 June 2000)

The magnetic excitations of the square-lattice spin-1/2 antiferromagnet and high-T<sub>c</sub> parent  $\text{La}_2\text{CuO}_4$  are determined using high-resolution inelastic neutron scattering. Sharp spin waves with absolute amplitudes in agreement with theory including quantum corrections are found throughout the Brillouin zone. The observed dispersion relation shows evidence for substantial interactions beyond the nearest-neighbor Heisenberg term, which are best understood in terms of a cyclic or ring exchange due to the strong hybridization path around the  $\text{Cu}_4\text{O}_4$  square plaquettes.

While there is consensus about the basic phenomenology - electron pairs with non-zero angular momentum, unconventional metallic behavior in the normal state, tendencies towards charge and spin density order - of the high temperature copper oxide superconductors, there is no agreement about the microscopic mechanism. After over a decade of intense activity, there is not even consensus as to the simplest “effective Hamiltonian”, which is a short-hand description of the motions and interactions of the valence electrons, needed to account for cuprate superconductivity. Because much speculation is centered on magnetic mechanisms for the superconductivity, it is important to identify the interactions among the spins derived from the unfilled  $\text{Cu}^{2+}$  *d*-shells. The present experiments show that there are significant (on the scale of the pairing energies for high-T<sub>c</sub> superconductivity) interactions coupling spins at distances beyond the 3.8 Å separation of nearest-neighbor  $\text{Cu}^{2+}$  ions. Cyclic or ring exchange due to a strong hybridization path around the  $\text{Cu}_4\text{O}_4$  squares (see Fig. 1A), from which the cuprates are built, provides the most natural explanation for the measured interactions.  $\text{CuO}_2$  planes are thus the second example of an important Fermi system (<sup>3</sup>He is the other [1]) where strong cyclic exchange terms have been measured.

Magnetic interactions are revealed through the wavevector dependence or dispersion of the magnetic excitations. In magnetically ordered materials, the dominant excitations are spin waves which are coherent (from site to site as well as in time) precessions of the spins about their mean values. The lower frame of Fig. 1B shows the dispersion relation calculated using conventional linear spin-wave theory in the classical large-*S* limit, where the only magnetic interaction is a strong nearest-neighbor superexchange coupling *J* [2]. We identify wavevectors by their coordinates (*h*, *k*) in the two-dimensional (2D) reciprocal space of the square lattice.

Spin waves emerge from the wavevector (1/2,1/2) characterizing the simple antiferromagnetic (AF) unit cell doubling in  $\text{La}_2\text{CuO}_4$  [3], and disperse to reach a maximum energy  $-2J$ - that is a constant along the AF zone boundary marked by dashed squares in Fig. 1B. Longer-range interactions manifest themselves most simply at the zone boundary. The upper frame of Fig. 1B shows the dispersion calculated with modest interactions between next nearest-neighbors. Virtually the only visible effect of the additional interactions is the dispersion of the spin waves along the zone edge. Thus, experiments to test for such interactions must measure the spin waves along the zone boundary. Only inelastic neutron scattering with high energy and wavevector resolution can accomplish this, although photon spectroscopy [4–7] has led to suspicions of such interactions.

For  $\text{La}_2\text{CuO}_4$ , a requirement that complicates meeting the resolution goals is the need to use neutrons with energies in the epithermal, 0.1–1.0 eV, range rather than in the more conventional cold and thermal [8], 2–50 meV, regimes. An early high energy neutron scattering experiment [9] revealed well-defined spin-wave excitations throughout the Brillouin zone which could be modeled using a nearest-neighbor Heisenberg exchange *J*=136 meV. The directions of the scattered neutrons were specified only to within the solid angle determined by the large detector dimensions. Thus, the measured spectra represented averages over large portions of the reciprocal space, so that dispersion along the zone boundary was unresolvable and only an upper bound could be placed on further neighbor couplings. The advance enabling the present investigation is the use of position-sensitive detectors for the scattered neutrons, which increases the wavevector resolution by an order of magnitude. The new detector bank is installed in the direct-geometry High-Energy Transfer (HET) time-of-flight spectrometer at the ISIS proton-driven pulsed neutron spallation source.

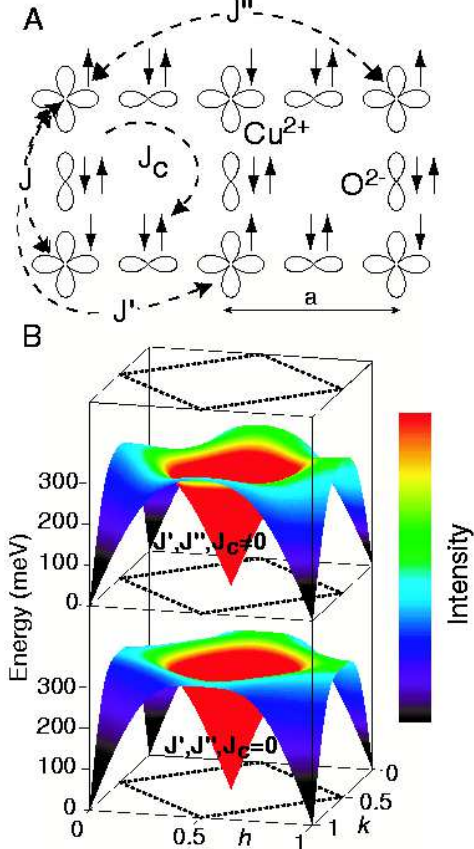


FIG. 1. (color) **A** The CuO<sub>2</sub> plane showing the atomic orbitals (Cu 3d<sub>x<sup>2</sup>-y<sup>2</sup></sub> and O 2p<sub>x,y</sub>) involved in the magnetic interactions.  $J$ ,  $J'$  and  $J''$  are the first-, second- and third-nearest-neighbor exchanges and  $J_c$  is the cyclic interaction which couples spins at the corners of a square plaquette. Arrows indicate the spins of the valence electrons involved in the exchange. **B** Lower surface is the dispersion relation for  $J=136$  meV and no higher-order magnetic couplings or quantum corrections. The upper surface shows the effect of the higher-order magnetic interactions determined by the present experiment. Colour is spin-wave intensity and includes the Cu<sup>2+</sup> 3d<sub>x<sup>2</sup>-y<sup>2</sup></sub> form factor.

Fig. 2A shows data in the form of constant energy scans for wavevectors around the antiferromagnetic zone center. As  $E$  increases, counter-propagating modes become apparent. As the zone boundary is approached and there is less dispersion, inspection of Fig. 1B reveals that it should be easier to locate the spin waves via energy scans performed at fixed wavevector. Fig. 2B shows a series of such scans collected at various points along the zone boundary. The spin waves have a clearly noticeable dispersion, from a minimum of  $282\pm 7$  meV near  $\mathbf{Q}=(3/4,1/4)$  to a maximum of  $318\pm 8$  meV near  $(1/2,0)$ . This is in obvious contrast to the dispersion-less behavior of linear spin-wave theory for the nearest-neighbor Heisenberg model. We have collected data throughout the Brillouin zone, and Fig. 3A shows the resulting dis-

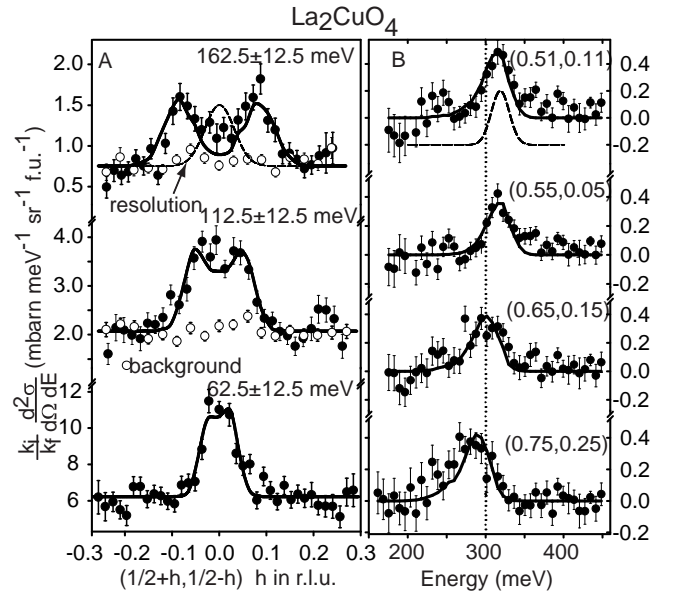


FIG. 2. Scattering from the spin waves in La<sub>2</sub>CuO<sub>4</sub>. Data result from 68 hours (A) and 221 hours (B) counting at a proton current of 170  $\mu$ A. The sample is described in [10]. Solid lines are fits to a spin-wave cross-section convolved with the instrumental resolution. (A) Const- $E$  cuts near the AF zone center for an incident energy  $E_i=250$  meV at  $T=295$  K.  $Q_z$  wavevector components at scan centers are  $l=2.8$  (bottom panel), 6.2 and 9.6 r.l.u. Open circles are a background measured near the (0,0) position. Dashed curve is the instrumental response to spin waves of infinite velocity. (B) Const- $Q$  cuts, with  $E_i=750$  meV, yield the dispersion along the AF zone boundary. Vertical dotted line at  $E=300$  meV is a guide to the eye.  $l$  values at peak position vary from 8.5 (bottom panel) to 9.6 (top panel). A background measured near the nuclear zone center (1,0) has been subtracted. Data showed are the average of the measurements at  $T=10$  K and 295 K which gave consistent peak positions and intensities. Dashed curve is the instrumental response to a dispersionless mode.

persion along major symmetry directions obtained from cuts of the type shown in Fig. 2. Fig. 3B displays the corresponding spin-wave amplitudes, in absolute units calibrated using acoustic phonon scattering from the sample.

To understand our results, we consider a Heisenberg Hamiltonian including higher order couplings [11–13]

$$\begin{aligned} \mathcal{H} = & J \sum_{\langle i,j \rangle} \mathbf{S}_i \cdot \mathbf{S}_j + J' \sum_{\langle i,i' \rangle} \mathbf{S}_i \cdot \mathbf{S}_{i'} + J'' \sum_{\langle i,i'' \rangle} \mathbf{S}_i \cdot \mathbf{S}_{i''} \\ & + J_c \sum_{\langle i,j,k,l \rangle} \{ (\mathbf{S}_i \cdot \mathbf{S}_j)(\mathbf{S}_k \cdot \mathbf{S}_l) + (\mathbf{S}_i \cdot \mathbf{S}_l)(\mathbf{S}_k \cdot \mathbf{S}_j) \\ & - (\mathbf{S}_i \cdot \mathbf{S}_k)(\mathbf{S}_j \cdot \mathbf{S}_l) \}. \end{aligned} \quad (1)$$

$J$ ,  $J'$  and  $J''$  are the first-, second- and third-nearest-neighbor exchanges where the paths are illustrated in Fig. 1A.  $J_c$  is the ring exchange interaction coupling four

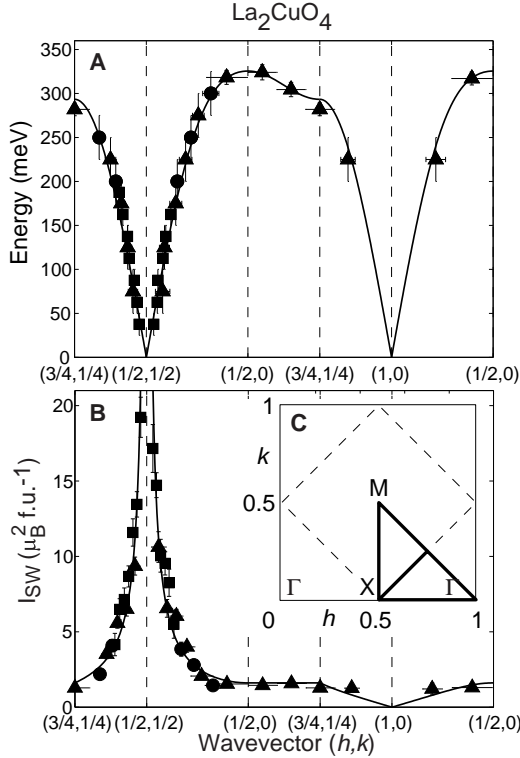


FIG. 3. (A) Dispersion relation along high symmetry directions in 2D Brillouin zone, see inset (C), at  $T=295$  K. Squares were obtained for  $E_i=250$  meV, circles for  $E_i=600$  meV and triangles for  $E_i=750$  meV. Points extracted from constant- $E$ -( $Q$ ) cuts have a vertical (horizontal) bar to indicate the  $E$ ( $Q$ ) integration band. Solid line is a fit to the spin-wave dispersion relation as discussed in the text. (B) Wavevector-dependence of the spin-wave intensity compared with predictions of linear spin-wave theory shown by the solid line. The absolute intensities yield a wavevector-independent intensity-lowering renormalization factor of  $0.52 \pm 0.13$  in agreement with the theoretical prediction 0.61 [14].

spins (labelled clockwise) at the corners of a square plaquette. Each spin coupling is counted once in Eq. (1). We first assume that only  $J$  and  $J'$  are significant i.e.  $J'' = J_c = 0$ . The solid lines in Fig. 2 are calculated using classical (large- $S$ ) linear spin-wave theory based on Eq. (1). As can be seen in the figures, the model provides an excellent description of both the spin wave amplitudes and energies. The nearest-neighbor exchange is antiferromagnetic,  $J=110.7 \pm 5$  meV, while the next-nearest-neighbor exchange across the diagonal is ferromagnetic,  $J'=-13.6 \pm 5$  meV (a wavevector-independent quantum renormalization factor [14] of the excitation energies,  $Z_c=1.18$ , was used in converting spin-wave energies into exchange couplings).

A ferromagnetic  $J'$  contradicts theoretical predictions [15], which give an antiferromagnetic superexchange  $J'$ . Wavevector-dependent quantum corrections [16] to the spin-wave energies can also lead to a dispersion along

the zone boundary even if  $J'=0$ , but with sign opposite to our result. Another problem with a ferromagnetic  $J'$  comes from measurements on  $\text{Sr}_2\text{Cu}_3\text{O}_4\text{Cl}_2$ . This material contains a similar exchange path between  $\text{Cu}^{2+}$  ions to that yielding  $J'$  in  $\text{La}_2\text{CuO}_4$  and analysis of the measured spin-wave dispersion leads to an antiferromagnetic exchange coupling for this path [17].

The neglect of all but the first two quadratic terms in Eq. (1) yields an excellent fit to our data, but gives an unphysical sign for  $J'$ . The validity of ignoring other terms must therefore be questioned, which we do by returning to the origin of further neighbor exchange, namely the coherent motion of electrons beyond nearest-neighbor sites [11–13]. Such processes can be described via the one-band Hubbard model [18] widely used as a starting point for theories of the cuprates,

$$\mathcal{H} = -t \sum_{\langle i,j \rangle \sigma=\uparrow\downarrow} (c_{i\sigma}^\dagger c_{j\sigma} + \text{H.c.}) + U \sum_i n_{i\uparrow} n_{i\downarrow}, \quad (2)$$

where  $\langle i,j \rangle$  stands for pairs of nearest-neighbors counted once. Eq. (2) has two contributions: the first is the kinetic term characterized by a hopping energy  $t$  between nearest-neighbor Cu sites and the second the potential energy term with  $U$  being the penalty for double occupancy on a given site. At half filling, the case for  $\text{La}_2\text{CuO}_4$ , there is one electron per site and for  $t/U \rightarrow 0$ , charge fluctuations are entirely suppressed in the ground state. The remaining degrees of freedom are the spins of the electrons localized at each site. For small but nonzero  $t/U$ , the spins interact via a series of exchange terms, as in Eq. (1), due to coherent electron motion touching progressively larger numbers of sites. If the perturbation series is expanded to order  $t^4$  (i.e. 4 hops), the exchange constants in Eq. (1) are [11–13]  $J = 4t^2/U - 24t^4/U^3$ ,  $J_c = 80t^4/U^3$  and  $J' = J'' = 4t^4/U^3$ . Using these expressions for the exchange constants and linear spin wave theory [19], we again fitted the dispersion and intensities of the spin-wave excitations. The fits are indistinguishable from those for variable  $J$  and  $J'$ . Again assuming [20]  $Z_c=1.18$ , we obtained  $t=0.32 \pm 0.02$  eV and  $U=2.6 \pm 0.3$  eV, in agreement with  $t$  and  $U$  determined from photoemission [21] and optical spectroscopy [22]. The corresponding exchange interactions are  $J=143.3 \pm 5$  meV and  $J'=48.4 \pm 9$  meV.

Many results on oxides of copper fall into place when cyclic exchange of the size that we measure is taken into account. First, the relative magnitude of the cyclic exchange  $J'/J = 0.34 \pm 0.06$  is consistent with the ratio of 0.30 estimated from numerical simulations [23] on finite clusters on the Cu-O square lattice. Second, magnetic Raman scattering [4,5] and infrared absorption experiments [6,7] show an unusual broadening towards higher energies that cannot be accounted for by a simple (quadratic) Heisenberg Hamiltonian, but can be attributed [5,6] to a cyclic term. Finally, in the related com-

pound  $\text{Sr}_{12}\text{Cu}_{24}\text{O}_{41}$ , which has square plaquettes stacked to form a ladder, the exchange constants corresponding to the nearly-equal-length rungs and legs of the ladder are 130 meV and 72 meV respectively [24] when no cyclic exchange is included. The inclusion of a ring exchange term [25]  $J_c = 34$  meV resolves the apparent inconsistency and allows the rungs and legs of the ladder to have similar exchange constants of 121 meV.

We have used a new high-wavevector-resolution epithermal-neutron scattering technique to discover that interactions beyond those coupling nearest-neighbor  $\text{Cu}^{2+}$  ions are needed to account for the magnetism of  $\text{La}_2\text{CuO}_4$ . The dominant further neighbor term is a four-spin cyclic interaction, which arises because the large orbital hybridization in the  $\text{CuO}_2$  planes provides an exchange path to include all four spins at the corners of elementary  $\text{Cu}_4\text{O}_4$  plaquettes. Thus,  $\text{La}_2\text{CuO}_4$  joins the nuclear magnet  $^3\text{He}$  [1] as a system where there is good evidence for substantial ring exchange. Ring exchange occurs even for very simple models, such as the single band Hubbard model, which contains only hopping ( $t$ ) and on-site Coulomb ( $U$ ) terms. We have determined  $t$  and  $U$  using only knowledge - in the form of our spin wave dispersion relation - of charge-neutral excitations and find values in excellent agreement with those obtained via charge-sensitive spectroscopies as well as numerical work on finite clusters. Thus, our results demonstrate that a one-band Hubbard model is an excellent starting point [26] for describing the magnetic interactions in the cuprates, and that even when considering relatively low energy spin excitations, charge fluctuations involving double occupancy must be taken into account. In addition, the scale of the cyclic exchange interactions, which are comparable to pairing energies in the high-T<sub>c</sub> materials, implies that they themselves or related electronic currents [27,28] might be important for superconductivity in the doped cuprates.

We are grateful to Risø National Laboratory for help in preparing this experiment and to J.F. Annett, H.-B. Braun, A.V. Chubukov, G. Sawatzky, Z-X. Shen and R.R.P. Singh for very helpful discussions. ORNL is managed for the US DOE by UT-Battelle, LLC, under contract DE-AC05-00OR22725.

[1] M. Roger, J.H. Hetherington, and J.M. Delrieu, *Rev. Mod. Phys.* **55**, 1 (1983).

[2] P.W. Anderson in *Magnetism*, eds. G.T. Rado and H. Suhl (Academic, New York, 1963), Vol. 1, p 25.

[3] D. Vaknin *et al.*, *Phys. Rev. Lett.* **58**, 2802 (1987).

[4] K.B. Lyons *et al.*, *Phys. Rev. B* **39**, 9693 (1989).

[5] S. Sugai *et al.*, *Phys. Rev. B* **42**, 1045 (1990).

[6] J. Lorenzana, J. Eroles, and S. Sorella, *Phys. Rev. Lett.* **83**, 5122 (1999).

[7] J.D. Perkins *et al.*, *Phys. Rev. Lett.* **71**, 1621 (1993).

[8] G. Shirane *et al.*, *Phys. Rev. Lett.* **59**, 1613 (1987).

[9] S.M. Hayden *et al.*, *Phys. Rev. Lett.* **67** 3622 (1991).

[10] The sample was an array of 7 mutually aligned single crystals with total mass 48.6 g. The crystals were annealed in argon atmosphere at 800°C for 2 hours to achieve the correct oxygen stoichiometry. The Néel temperature, measured via elastic neutron scattering, was  $325 \pm 5$  K, consistent with the highest values in the literature [29].

[11] M. Takahashi, *J. Phys. C :Solid State Phys.* **10**, 1289 (1977).

[12] M. Roger and J.M. Delrieu, *Phys. Rev. B* **39**, 2299 (1989).

[13] A.H. MacDonald, S.M. Girvin, and D. Yoshioka, *ibid* **41**, 2565 (1990).

[14] R.R.P. Singh, *Phys. Rev. Lett.* **39**, 9760 (1989).

[15] J.F. Annett *et al.*, *Phys. Rev. B* **40**, 2620 (1989).

[16] C.M. Canali, S.M. Girvin, and M. Wallin, *Phys. Rev. B* **45**, 10131 (1992); R.R.P. Singh and M.P. Gelfand, *ibid* **52**, 15695 (1995).

[17] Y.J. Kim *et al.*, *Phys. Rev. Lett.* **83**, 852 (1999).

[18] J. Hubbard, *Proc. R. Soc. London, Series A* **276**, 238 (1963).

[19] A.V. Chubukov, E. Gagliano, and C. Balseiro, *Phys. Rev. B* **45**, 7889 (1992).

[20] Including the effect of the wavevector-dependence [16] of the quantum renormalization factor  $Z_c$  is expected to modify slightly the extracted values of all exchange parameters leading to a larger  $J_c$ . Accurate determinations require extending the calculation of  $Z_c(\mathbf{Q})$  for the nearest-neighbor model [16] to the case of finite higher-order terms as in Eq. (1).

[21] C. Kim *et al.*, *Phys. Rev. Lett.* **80**, 4245 (1998).

[22] H.-B. Schüttler and A.J. Fedro, *Phys. Rev. B* **45**, 7588 (1992).

[23] H.J. Schmidt and Y. Kuramoto, *Physica C* **167**, 263 (1990); Y. Mizuno, T. Tohyama, and S. Maekawa, *J. Low. Temp. Phys.* **117**, 389 (1999).

[24] R.S. Eccleston *et al.*, *Phys. Rev. Lett.* **81**, 1702 (1998).

[25] S. Brehmer *et al.*, *Phys. Rev. B* **60**, 329 (1999).

[26] P.W. Anderson, *Science* **235**, 1196 (1987).

[27] T.C. Hsu, J.B. Marston and I. Affleck, *Phys. Rev. B* **43**, 2866 (1991).

[28] C.M. Varma, *Phys. Rev. B* **55**, 14554 (1997).

[29] B. Keimer *et al.*, *Phys. Rev. B* **46**, 14034 (1992).

---

[1] M. Roger, J.H. Hetherington, and J.M. Delrieu, *Rev. Mod. Phys.* **55**, 1 (1983).

[2] P.W. Anderson in *Magnetism*, eds. G.T. Rado and H. Suhl (Academic, New York, 1963), Vol. 1, p 25.

[3] D. Vaknin *et al.*, *Phys. Rev. Lett.* **58**, 2802 (1987).

[4] K.B. Lyons *et al.*, *Phys. Rev. B* **39**, 9693 (1989).

[5] S. Sugai *et al.*, *Phys. Rev. B* **42**, 1045 (1990).

[6] J. Lorenzana, J. Eroles, and S. Sorella, *Phys. Rev. Lett.*